

A Novel Micro-G Emulation System Using Active Magnetic Compensator for Complex Space Operations

Tao Wen^{1, *}, Zhengfeng Ming¹, Zhanxia Zhu^{2, 3}, Wenzhi Zhu¹, and Shuang Ning¹

Abstract—To perform the ground simulation experiments of the complex space operations, this work proposes a new active magnetic suspension compensator. The large-gap magnetic suspension compensator (LGMSC) is a conceptual design for a ground-based experiment which could be used to investigate the technology issues associated with accurate suspended element control at large gaps. This compensator can be used as the out-of-plane electromagnetic actuator for the 3-DOF fine stage in certain high precision positioning applications. Based on the equivalent current method, we explain the basics of the magnetic suspension compensator and analyze its advantages. A gravity compensator has been realized in a test setup that shows the feasibility of the chosen modeling technique and of magnetic gravity compensation.

1. INTRODUCTION

As a new frontier in spatial science, the experiment under microgravity is one of the essential steps for verifying the space enabling technologies on the ground [1]. The test and demonstration of complex space operations require that the ground test system should provide a long-duration, large-scale, accurate, controllable and almost real microgravity test environment to simulate the space motion in the same degree as in space.

Currently, there are two types of simulation methods. The first is the environment simulation method, including the Zero-G airplane and the drop tower; the second is the effect simulation method that maintains the apparent gravity of the tested-body continually to be zero, including the airbearing suspension system, the sling suspension system and the neutral buoyancy system. Due to some shortages of the present methods, none can perfectly meet the above-mentioned requirements [1–5].

In addition to the above-mentioned methods, there are many other facilities and methods for simulating the weightless environment or some biological effects under the weightless condition. However, most of the methods are used for research on microscopic substances instead of macroscopic bodies. The above analysis shows that, to carry out experiments of spatial operations on the ground, the existing microgravity simulation methods have their own drawbacks, being unable to satisfy all requirements [6–14]. To well address the issues, our research team have firstly put forward an innovative method based on hybrid compensation, its basic principle is the combination of magnetic compensation and neutral buoyancy, which was proposed in [2]. The core of this method is the active magnetic suspension compensator for the moving actuator.

Related research projects on passive magnetic levitation and gravity compensation have been discussed in a number of papers. A new magnetic gravity compensation system using permanent magnets and a Lorentz coil was proposed in [15]. In [16] and [17], a flat-type active magnetic bearing using Halbach magnet arrays and Lorentz coils for a magnetic levitation stage was proposed. Large

Received 22 August 2016, Accepted 21 October 2016, Scheduled 4 November 2016

* Corresponding author: Tao Wen (xidiantwt2012@163.com).

¹ School of Electronic & Mechanical Engineering, Xidian University, Xi'an, Shaanxi 710071, China. ² School of Astronautics, Northwestern Polytechnical University, Xi'an 710072, China. ³ National Key Laboratory of Aerospace Flight Dynamics, 127 West Youyi Road, Xi'an 710072, China.

forces and low stiffness could be achieved through design optimization. In [18], a magnetic levitation table supported by repulsive forces of four sets of permanent magnets was researched. In [19], the design criteria and parameter optimization of a quasi-zero stiffness magnetic levitation system were presented. An electromagnetic isolator for gravity compensation of a heavy payload by active permanent magnetic force was designed in [20]. In [21], improved 3-D analytical expression for the torque between the permanent magnets in magnetic bearings was derived by using the Lorentz force method. In [22], unequal magnet arrays were adopted in a magnetic gravity compensator to realize the goal of a large active force and low stiffness.

Precision positioning in multi-degrees-of-freedom is usually required in many advanced industrial applications. In order to compensate for the moving actuator, mechanical springs, air bearings, and magnetic levitation have been discussed. Among these methods, the mechanical spring is subject to mechanical coupling, which limits the positioning accuracy of the fine stage. Air bearing is a good choice for gravity compensation because of its stable characteristics and mature technologies. However, the system structure will be very complex if a high experimental condition is required. In contrast, magnetic levitation has many advantages, such as no mechanical contact, high force density, experimental environment compatibility, and structure simplicity.

In this paper, a novel rectangular large-gap magnetic suspension compensator (LGMSC) is proposed, which can be used as the z actuator for the fine stage [23–32]. The LGMSC provides an integrated solution involving active gravity compensation and positioning control by employing active magnetic levitation embedded with Lorentz coil array, and the permanent magnet is applied in the mover. Although the magnetic suspension technology is widely adopted in many types of motors and actuators, a special problem will occur when it is applied under large air-gap. However, to date, this application has not been well researched. The primary contribution of this paper is to analyze the leading cause of the mentioned problem and to propose an improved magnetic suspension compensator to perform the ground simulation experiments of the complex space operations.

This paper is organized as follows. In Section 2, the structure and principle of the LGMSC are proposed and the traditional analytical model for the LGMSC is established. In Section 3, we propose an improved semianalytical model in which the actual difference in the operating points of the moving magnet is considered. Then, the characteristics of the electromagnetic force and magnetic field distribution are also analyzed based on the finite-element method. In Section 4, the relevant experimental verification is completed.

2. CONCEPT DESIGN

2.1. System Design

The gravity compensation ground-based experiment system, as originally defined, is shown schematically in Figure 1. It consists of a cylindrical suspended element which has a core composed of permanent

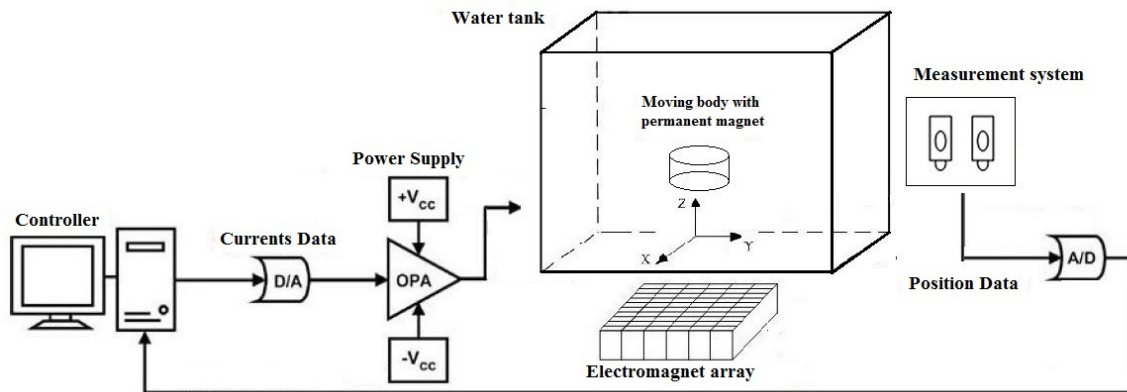


Figure 1. Schematic representation of the proposed system.

magnet material embedded in it. Most of the levitation forces are produced by neutral buoyancy, and the control force are produced by electromagnet array which are required to closely fit in a horizontal plane, and the axis direction of each component is made to parallel with each other and be perpendicular to the horizontal plane. The structure and performance of each excitation coil component is consistent.

As shown in the Figure 1, the magnetization vector of the permanent magnet is vertical. By adjusting the persistent-mode currents to the correct values, a vertical field and gradient can be produced at the location of the electromagnet coil which will produce a stable levitation force. Required control forces are provided by the separate control coils.

In addition to the system control, the suspended element also contains an array of LEDs and associated electronics and power supply. The LEDs are embedded in the surface of the suspended element and provide active targets for a photogrammetric optical position measurement system. Position and orientation of the model is determined from the position of the projected garget images.

2.2. Dynamics Analysis

The translational acceleration of the suspended-load \vec{a} can be written as:

$$\{\vec{a}\} = (1/m) \{\vec{F}\} \quad (1)$$

where m is the mass of the suspension load, and \vec{F} denotes the total force on the suspended-load.

$$\{\vec{F}\} = \{\vec{F}_b\} + \{\vec{F}_m\} + \{\vec{F}_d\} + \{\vec{F}_g\} \quad (2)$$

where \vec{F}_b denotes the buoyancy, \vec{F}_m the control forces produced by the electromagnets, \vec{F}_d the external disturbance force, and \vec{F}_g the force of gravity. In a microgravity environment, the ideal state of the object is:

$$\{\vec{F}\} = 0 \quad (3)$$

In the proposed microgravity environment, the suspended element can move in a wide range of the three-dimensional space. Hence, the only control purpose is without affecting the suspended-load's own motion control. This invention relates to the suspension of a suspended element in space by magnetic levitation and more particularly to the use of the electromagnet array which are symmetrically positioned about a central vertical axis, and are selectively energized, for providing both lift and directional stability to the object.

In the control process, the distribution form of the excitation coil array is mainly according to the position of the suspended-load. For the experiment system, the electromagnetic force at different height should be a reference. Considering the disturbance from the posture change of the suspended-load, we treat load current, horizontal and vertical movement as the input variables. The basic idea is: when the suspended-load does any irregular movement, we decouple the movement process into horizontal and vertical movements. Meanwhile, we track it in real-time and collect its trajectory.

2.3. Ground-Space Similarity

Note that it is relatively easy to achieve the geometrical similarity, but difficult to achieve the experimental environment similarity, especially the mechanical environment similarity. Compared with spatial microgravity environment, in addition to gravity, buoyancy and electromagnetic force are introduced artificially in the ground experimental environment. Under the free-floating condition, the gravity, buoyancy, electromagnetic force and environmental disturbance act on the tested-body. Hence, for the sake of the mechanical environment similarity, the tested-body must stay in suspension (equilibrium) and constant orientation (moment equilibrium) at any position.

3. ANALYSIS MODEL OF MAGNETIC

3.1. Electromagnet Force Model Analysis

The equations for forces on a permanent magnet which are produced by electromagnet array have been presented and discussed in the following section. The force on a permanent magnet, in a given orthogonal x, y, z coordinate system. The force can be written as:

$$\{F_m\} = \int (d\{M\} \cdot \nabla) \{B\} dV \quad (4)$$

Where Vol is the volume of the core, B calculated at the center of the core, and M the magnetization of the permanent.

Since the size of the suspended element is small relative to the size of the electromagnets and the gaps involved, a reasonable approximation of the forces which are produced can be obtained by making the assumption that the field and gradient components are uniform over the volume of the coil. Under this assumption:

$$\{M\} \cdot \nabla = \{M\}^T \nabla = \left(M_x \frac{\partial}{\partial x} + M_y \frac{\partial}{\partial y} + M_z \frac{\partial}{\partial z} \right) \quad (5)$$

Taking the dot product, $\{M\} \cdot \nabla$ results in the scalar. Equation (4) then becomes:

$$\{F_m\} = (Vol) \begin{bmatrix} M_x \frac{\partial B_x}{\partial x} + M_y \frac{\partial B_x}{\partial y} + M_z \frac{\partial B_x}{\partial z} \\ M_x \frac{\partial B_y}{\partial x} + M_y \frac{\partial B_y}{\partial y} + M_z \frac{\partial B_y}{\partial z} \\ M_x \frac{\partial B_z}{\partial x} + M_y \frac{\partial B_z}{\partial y} + M_z \frac{\partial B_z}{\partial z} \end{bmatrix} \quad (6)$$

The notation can be simplified considerably by letting B_{ij} represent $\partial B_i / \partial j$. By factoring M out as a vector, (6) can be written in the form

$$\{F_m\} = (Vol) [\partial B] \{M\} \quad (7)$$

Where

$$\{\partial B\} = \begin{bmatrix} B_{xx} & B_{xy} & B_{zx} \\ B_{yx} & B_{yy} & B_{zy} \\ B_{zx} & B_{xy} & B_{zz} \end{bmatrix} \quad (8)$$

in simplified notation. From Maxwell's equations, in the region of the core, $\nabla \times B = 0$ which results in

$$B_{xy} = B_{yx} \quad B_{xz} = B_{zx} \quad B_{yz} = B_{zy} \quad (9)$$

Also $\nabla \cdot B = 0$ which results in

$$B_{xx} + B_{yy} + B_{zz} = 0 \quad (10)$$

The magnetic force becomes

$$\{\vec{F}_m\} = Vol [T_m] [\partial B] [T_m]^{-1} \{\vec{M}\} \quad (11)$$

The translational acceleration of the suspension load, in coil coordinates, can be written as:

$$\{\vec{a}\} = (1/m) \left(Vol \left([T_m] [\partial B] [T_m]^{-1} \{\vec{M}\} \right) + \{\vec{F}_d\} \right) \quad (12)$$

Where m is the mass of the suspended element, Vol the volume of the load, \vec{M} the magnetization of the suspended element, T_m the vector transformation matrix from inertial to load coordinates, B the flux density produced by the electromagnets, and \vec{F}_d the external disturbance forces in load coordinates.

Since the fields and gradients are linear functions of coil currents, the components of \vec{B}_z produced by coil n of an n -coil of $n \times n$ array can be written as:

$$\vec{B}_{zn} = K_n \left(\frac{I_n}{I_{\max}} \right) \quad (13)$$

Where I_{\max} is the maximum coil current, k_n a constant which represents the magnitude of \vec{B}_{zn} produced by I_{\max} , and I_n the coil current. For the total system, \vec{B}_z can be written as:

$$\vec{B}_z = \left(\frac{1}{I_{\max}} \right) [K_x] \{I\} \tag{14}$$

where

$$[K_z] = [K_{z1} \quad K_{z2} \quad \dots \quad K_{zn}]. \tag{15}$$

And

$$[I]^T = [I_1 \quad I_2 \quad \dots \quad I_n]. \tag{16}$$

The gradients can be put in the same form by arranging the elements of ∂B as a column vector. This results in

$$\{\partial B\} = (1/I_{max}) [K_{\partial B}] \{I\} \tag{17}$$

where ∂B is a nine element column vector containing the gradients of $\{B\}$ and is a $9 \times n$ matrix whose elements represents the values of ∂B produced by a corresponding coil driven by the maximum current. Each element of ∂B , for example, can be written in the form

$$B_{xx} = (1/I_{max}) [K_{xx}] \{I\} \tag{18}$$

where $[K_{\partial B}]$ is a $1 \times n$ matrix containing values of B_{xx} produced by a corresponding coil driven by the maximum current.

This model is nonlinear because of the coordinate transformations and is of the form

$$\dot{q} = f(q, u) \tag{19}$$

where q is given by

$$q^T = [x, y, z]. \tag{20}$$

And the input u is given by

$$u^T = [I_1 \quad I_2 \quad \dots \quad I_n]. \tag{21}$$

3.2. Characteristics Analysis

The analytical solution of the 3D diffusion equation in the presence of moving conductors presents serious difficulties even in simple cases. When complex geometries and nonlinear materials are present, an accurate analysis can be performed by numerical methods only. To analyze the characteristics of model above, the finite-element model of the LGMSC is established using commercial finite-element software — ANSYS Maxwell.

The requirements for the LGMSC are given in Table 1. Through structural parameter optimization, the initial dimensions of the LGMSC can be determined and are shown in Table 2. In the finite-element model, the permanent magnet rings are NdFeB35 with $H_{cb} = -890000$ A/m, $B_r = 1.23$ T, and $\mu_r = 1.0998$.

The relationships between the force and system parameters based on the Finite Element Method are shown in Figure 2. We can see that the electromagnet force is proportional to the inverse square of the suspension height, and in a linear relationship other three parameters. When the suspension gap increases (especially reach meter level), some parameters have different relationship with the force compared with traditional formula. These results are useful for the system design and precise control.

Table 1. Requirement for the LGMSC.

<i>Item</i>	<i>Value</i>	<i>Unit</i>
Levitation force restriction	> 20	N
Motion range	(±1, ±1, 1)	m
Mover mass	1	kg
Current density of coils	5	A/mm ²

Table 2. Geometric parameters of the finite-element model.

<i>Item</i>	<i>Value</i>	<i>Unit</i>
Radius of the permanent magnet	50	mm
Thickness of the permanent magnet	30	mm
Side length of the coil	100	mm
width of the coil	50	mm
Thickness of the coil	100	mm

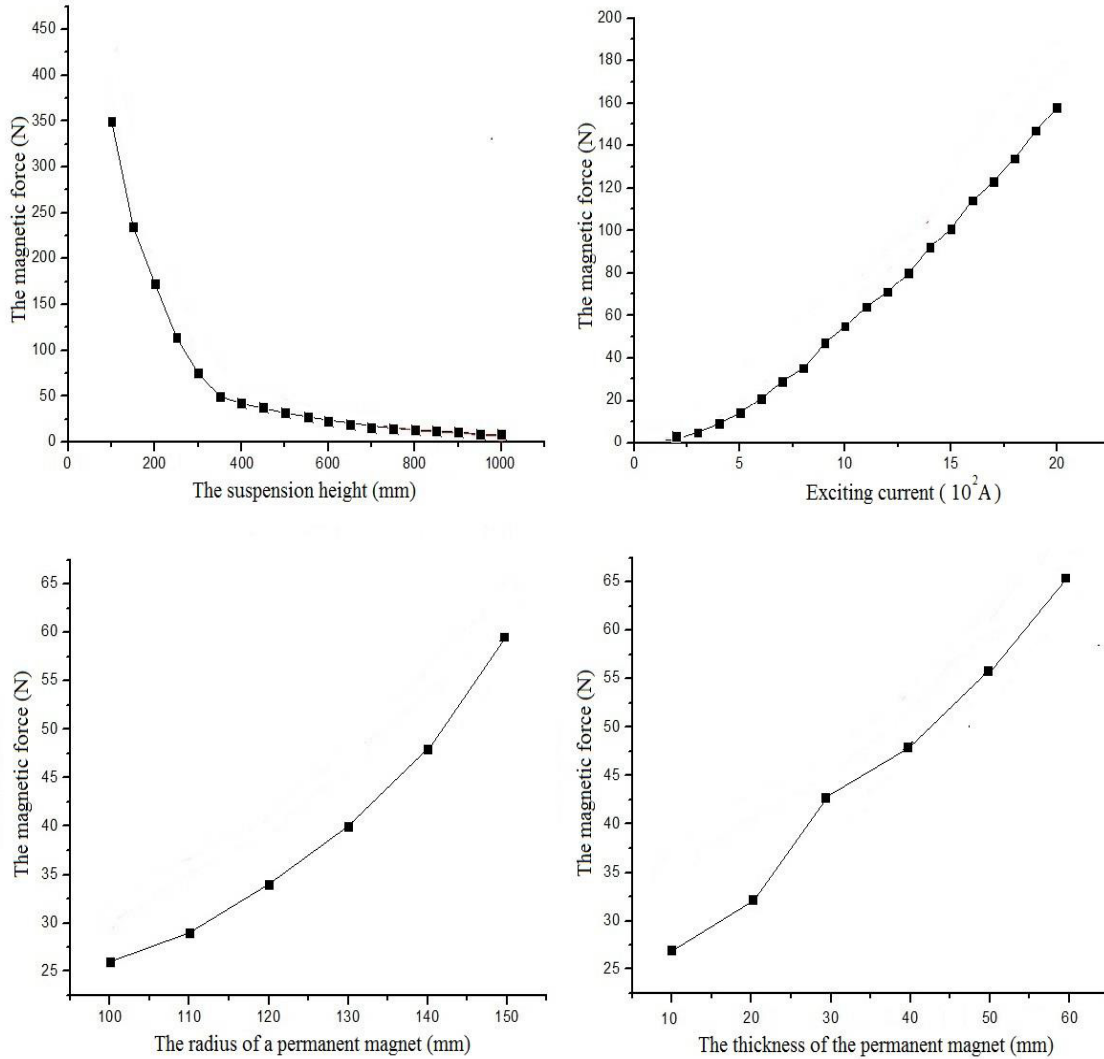


Figure 2. The electromagnetic force with different parameters.

Figure 3 shows the magnetic field distribution of the LGMSC (without permanent magnet). The homogenized magnetic field in the air gap is generated from the coil array. And by changing the input current, vertical magnetic field strength is also controllable. So we can realize three-dimensional equivalent magnetic compensation through this feature.

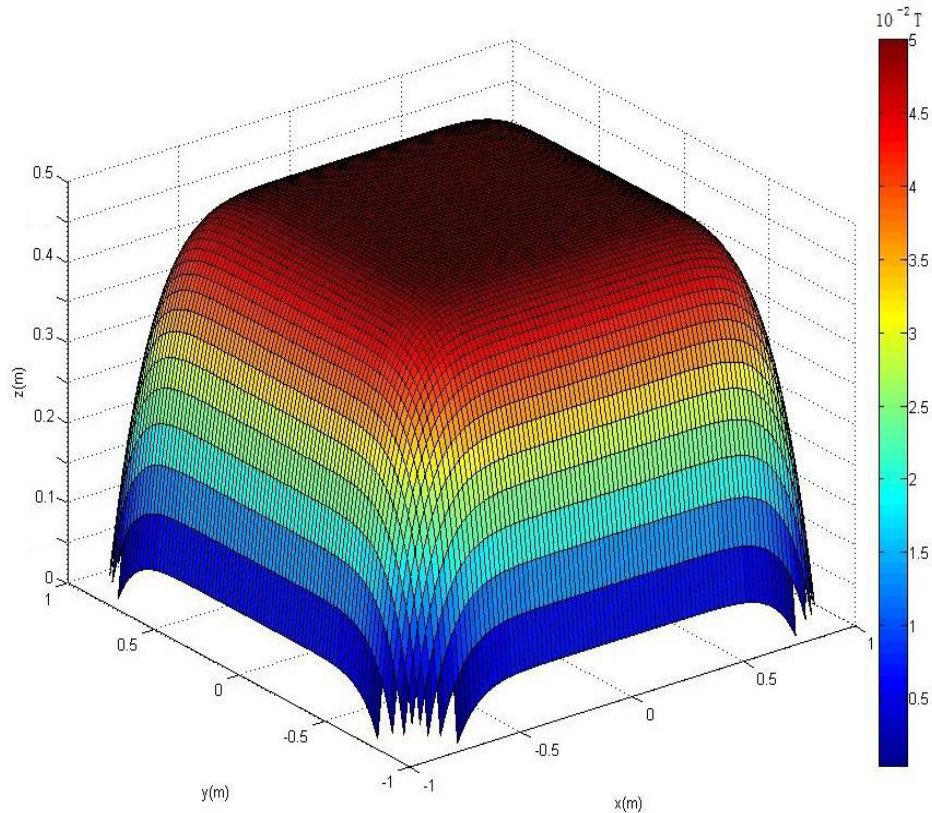


Figure 3. Magnetic field distribution of the LGMSC (without the permanent magnet).

4. EXPERIMENT VERIFICATION

Based on our innovative method, an experimental system has been built in our laboratory. Currently, the tested-body is a polyhedron with 26 surfaces. Six propeller thrusters, divided into three groups, are symmetrically mounted along three axes of the tested body respectively. Its buoyancy can reach approximately 101% G (in this case, the buoyancy is bigger than gravity) after being balanced by the liquid-float system, where the electromagnetic force accounts for about 1% of gravity. The distributed electromagnet array adopted here is 20×20 . After adjusting the direction of direct current, electromagnetic suction is generated and used for accurate balancing. After adjusting the size of electromagnetic force, the tested-body is able to stay stably suspended at a given position.

In order to verify the performance of the proposed method, the experimental platform of an experimental verification system has been built in our laboratory, as shown in Fig. 4.

Experiments have been conducted at several different depths. The electromagnetic force closed-loop control is applied to these depths until the tested-body gets stable, and then the sizes of current and voltage are recorded and kept constant. After this, the microgravity level is measured with the z -directional acceleration velocity of the tested-body (parallel to the local gravitational acceleration) and is measured by a standard accelerometer. Here, a sufficiently accurate accelerometer should be selected for the accuracy measurement of the microgravity of the tested-object, and the acceleration velocity measurement accuracy is 5×10^{-5} g at least.

Record the data in the process of the whole experiment. The microgravity level is measured with the z -directional acceleration velocity of the suspended-load (parallel to the local gravitational acceleration). The results at the height of 750 mm are described. As shown in Fig. 4 and Fig. 5, the microgravity level of the hybrid suspension system reaches up to 10^{-4} G and target is in a state of force balance in the vertical direction.

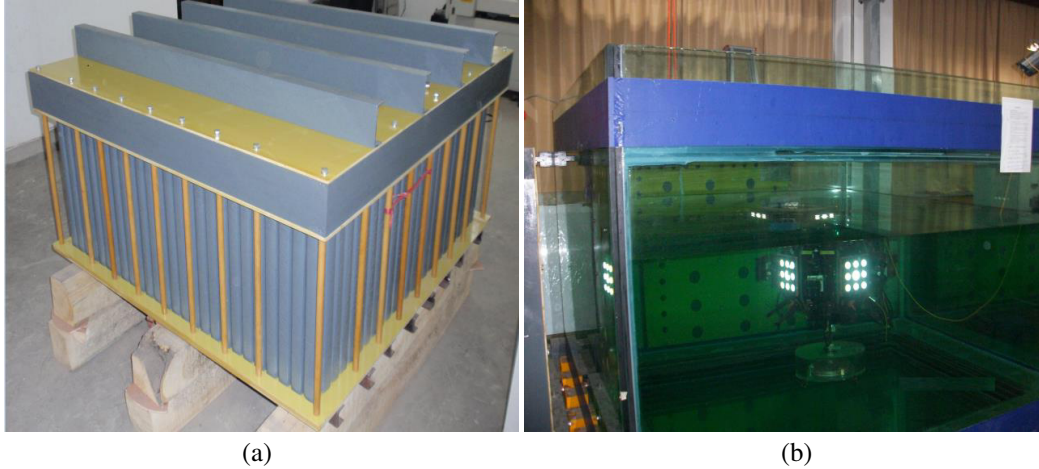


Figure 4. Experimental verification platform. (a) Electromagnet array. (b) The experimental test environment.

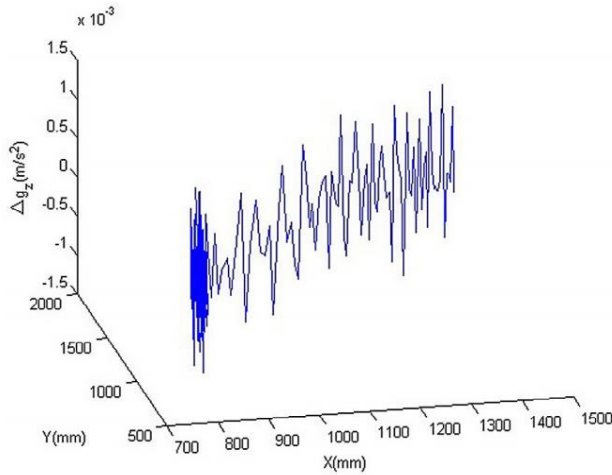


Figure 5. The micro-G test in hybrid suspension system.

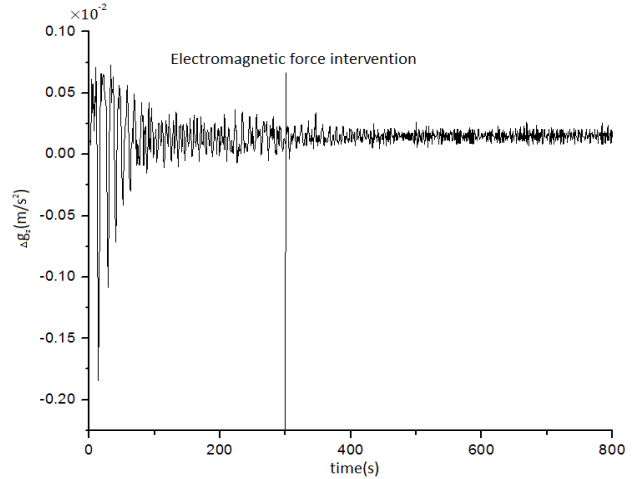


Figure 6. The change of micro-G in the experiment.

As a result, the above experiments show that the proposed simulation methods can improve the steady state and dynamic performance of microgravity and finally achieve the best experiment result.

5. CONCLUSIONS

Active magnetic gravity compensation method presents a powerful alternative to the classical low-gravity experimentation methods involving fluids, and this method can remedy not only the disadvantages of pure liquid-float simulation such as low accuracy and poor real-time adjustment but also the disadvantages of air-bearing simulation such as not enough DOFs of motion in a vertical direction.

This technology has potential applications in a wide range of areas including magnetically suspended pointing mounts for advanced actuators, and remote manipulation/control/positioning of objects in space. The proposed system seems to be able to satisfy the requisite of a functional simulation system. To sum up, the main contribution of this paper is the design of a new structure for a high-precision and long-range motion positioner, which successfully demonstrates feasibility and effectiveness of such a new system through extensive experimental results.

On the basis of our experimental verification system, the research on the following experimental and applied technologies can be undertaken, including recognition and test technologies of close-distance and non-cooperative targets, close-distance relative autonomous navigation technology and experimental technology, test of autonomous rendezvous approaching trajectory planning algorithm and its experimental technology, test of autonomous rendezvous approaching navigation and control method and its experimental technology, the motion control experimental technology with multiple DOFs for robot arms, research on the experimental technology of the 3-dimensional capture and release of a manipulator, research on new-concept spatial operation experiment technology, etc. These are also our main research interests in the future.

ACKNOWLEDGMENT

This study was supported by the National High Technology Research and Development Program of China (Grant No. 2015AA7041003) and the Fundamental Research Funds for the Central Universities (Grant No. JB150410). We also thank to the Chinese National Key Laboratory of Aerospace Flight Dynamics for technical support.

REFERENCES

1. Zhu, Z. and J. Yuan, *Test Facilities for Micro-G Effects of Spacecraft Operation*, China Astronautic Publishing House, 2013 (in Chinese).
2. Yuan, J. and Z. Zhu, "An innovative method for simulating microgravity effects through combining electromagnetic force and buoyancy," *Advances in Space Research*, Vol. 56, No. 2, 355–364, Jul. 15, 2015.
3. Akin, D. L., M. Bowden, and J. Spofford, "Neutral buoyancy evaluation of technologies for space station external operation," *The 35th Congress of the International Astronautical Federation*, 84–88, 1984.
4. Brown, H. B. and J. M. Dolan, "A novel gravity compensation system for space robots," *Proceedings of the ASCE Specialty Conference on Robotics for Challenging Environments*, 250–258, 1994.
5. Chappell, S. P., J. R. Norcross, and K. G. Clowers, "Final report of the integrated parabolic flight test: effects of varying gravity, center of gravity, and mass on the movement biomechanics and operator compensation of ambulation and exploration tasks," NASA/TP-2010-21637, 2010.
6. Viswanathan, S. P., A. Sanyal, and L. Holguin, "Dynamics and control of a six degrees of freedom ground simulator for autonomous rendezvous and proximity operation of spacecraft," *Proceedings of AIAA Guidance, Navigation, and Control Conference*, 2012–4926, 2012.
7. Quettier, L., H. Félice, A. Mailfert, D. Chatain, and D. Beysens, "Magnetic compensation of gravity forces in liquid/gas mixtures: surpassing intrinsic limitations of a superconducting magnet by using ferromagnetic inserts," *Eur. Phys. J. Appl. Phys.*, Vol. 32, 167–175, 2005.
8. Cheng, Z., "Neutral buoyancy microgravity environment simulation technology," *Spacecraft Environment Engineering*, Vol. 1, 1–6, 2000.
9. Wunenburger, R., D. Chatain, Y. Garrabos, and D. Beysens, "Magnetic compensation of gravity forces in (p-) hydrogen near its critical point: Application to weightless conditions," *Phys. Rev. E*, Vol. 62, 469–476, 2000.
10. Qi, N., "The primary discussion for the ground simulation system of spatial microgravity," *Aerospace Control*, Vol. 29, No. 3, 95–100, 2011.
11. Matunaga, S., "Micro-gravity experiments of space robotics and space-used mechanisms at Tokyo Institute of Technology," *J. Jpn. Soc. Microgravity Appl.*, Vol. 19, 101–5, 2002.
12. Han, O., D. Kienholz, P. Janzen, S. Kidney, "Gravity-offloading system for large-displacement ground testing of spacecraft mechanisms," *Proceedings of 40th Aerospace Mechanisms Symposium*, 119–132, NASA Kennedy Space Center, Florida, CA, May 12–14, 2010.
13. Chen, S. F., T. Mei, T. Zhang, and X. H. Wang, "Design of the controller for a crowd simulation system of spatial microgravity environment," *Robot*, Vol. 30, No. 3, 201–4, 2008 (Chinese).

14. Cheng, Z., "Neutral buoyancy microgravity environment simulation technology," *Spacecraft Environment Engineering*, Vol. 1, 1–6, 2000.
15. Hol, S. A. J., E. Lomonova, and A. J. A. Vandenput, "Design of a magnetic gravity compensation system," *Precis. Eng.*, Vol. 30, No. 3, 265–273, Jul. 2006.
16. Choi, Y. M., M. G. Lee, D. G. Gweon, and J. Jeong, "A new magnetic bearing using Halbach magnet arrays for a magnetic levitation stage," *Rev. Sci. Instrum.*, Vol. 80, No. 4, Art. ID. 045106, Apr. 2009.
17. Choi, Y. M. and D. G. Gweon, "A high-precision dual-servo stage using Halbach linear active magnetic bearings," *IEEE/ASME Trans. Mechatronics*, Vol. 16, No. 5, 925–931, Oct. 2011.
18. Choi, K. B., Y. G. Cho, T. Shishi, and A. Shimokohbe, "Stabilization of one degree-of-freedom control type levitation table with magnet repulsive forces," *Mechatronics*, Vol. 13, No. 6, 587–603, Jul. 2003.
19. Robertson, W. S., M. R. F. Kidner, B. S. Cazzolato, and A. C. Zander, "Theoretical design parameters for a quasi-zero stiffness magnetic spring for vibration isolation," *J. Sound Vib.*, Vol. 326, No. 1, 88–103, Sep. 2009.
20. Ding, C., J. L. G. Janssen, A. A. H. Damen, and P. P. J. van den Bosch, "Modeling and control of a 6-DOF contactless electromagnetic suspension system with passive gravity compensation," *Proc. 19th Int. Conf. Elect. Mach.*, 1–6, Rome, Italy, Sep. 6–7, 2010.
21. Janssen, J. L. G., J. J. H. Paulides, J. C. Compter, and E. A. Lomonova, "Three-dimensional analytical calculation of the torque between permanent magnets in magnetic bearings," *IEEE Trans. Magn.*, Vol. 46, No. 6, 1748–1751, Jun. 2010.
22. Janssen, J. L. G., J. J. H. Paulides, E. A. Lomonova, B. Delinchant, and J. P. Yonnet, "Design study on a magnetic gravity compensator with unequal magnet arrays," *Mechatronics*, Vol. 23, No. 2, 197–203, Mar. 2013.
23. Nabeel, A. S. and B. Amitave, "Electropermanent suspension system for acquiring large air-gaps to suspend loads," *IEEE Tran. on Mag.*, Vol. 6, No. 31, 4193–4195, 1995.
24. Bekinal, S. I., T. R. Anil, and S. Jana, "Analysis of axially magnetized permanent magnet bearing characteristics," *Progress In Electromagnetics Research B*, Vol. 44, 327–343, 2012.
25. Ausserlechner, U., "Closed analytical formulae for multi-pole magnetic rings," *Progress In Electromagnetics Research B*, Vol. 38, 71–105, 2012.
26. Babic, S. and C. Akyel, "Magnetic force between inclined circular loops (Lorentz approach)," *Progress In lectromagnetics Research B*, Vol. 38, 333–349, 2012.
27. Ravaud, R., G. Lemarquand, and V. Lemarquand, "Halbach structures for permanent magnets bearings," *Progress In Electromagnetic Research M*, Vol. 14, 263–277, 2010.
28. Janssen, J. L. G., J. J. H. Paulides, and E. A. Lomonova, "Study of magnetic gravity compensator topologies using an abstraction in the analytical interaction equations," *Progress In Electromagnetics Research*, Vol. 128, 75–90, 2012.
29. Morishita, M., T. Azukizawa, and S. Kanda, "A new maglev system for magnetically levitated carrier system," *IEEE Transactions on Vehicular Technology*, Vol. 38, No. 4, Nov. 1989.
30. White, G. C. and Y. S. Xu, "An active vertical-direction gravity compensation system," *IEEE Transactions on Instrumentation and Measurement*, Vol. 43, No. 6, 786–792, 1994.
31. Golob, M. and B. Tovornik, "Modeling and control of the magnetic suspension system," *ISA Transactions*, Vol. 42, No. 1, 89–100, 2003.